

T. YILDIZ\*, A. KAYA GÜR\*

**MICROSTRUCTURAL CHARACTERISTIC OF N<sub>2</sub> SHIELDING GAS IN COATING FeCrC COMPOSITE TO THE SURFACE OF AISI 1030 STEEL WITH PTA METHOD****WPŁYW ZAWARTOŚCI AZOTU W GAZIE OSŁONOWYM NA MIKROSTRUKTURĘ POWŁOK FeCrC NA STALI AISI 1030 OTRZYMANÝCH METODĄ NAPYLANIA PLAZMOWEGO**

In this study, FeCrC powder was alloyed on the surface of AISI 1030 steel with FeCrC powder having 70% Cr ratio with the Plasma Transferred Arc Welding Method. In the coating process performed with the Plasma Transferred Arc Welding Method, N<sub>2</sub> gas at 1-3-5% ratio was added to the shielding gas. The coating layer was analysed using optical microscope (OM), scanning electron microscope (SEM), X-ray diffractogram (XRD) and X-ray energy dispersive spectrometer (EDS). As a result of optical microscope and microstructure analyses, it was determined that the coating layer and the sub-layer were connected to each other metallurgically and there were austenite ( $\gamma$ ), Fe-Cr, Fe<sub>23</sub>(C)<sub>6</sub>, and Cr<sub>7</sub>C<sub>3</sub> phase and carbides and CrN in the structure.

*Keywords:* Plasma transferred arc coating; surface modifications; chromium carbide; chromium nitrides; microstructure

W pracy badano nakładanie powłok z proszku FeCrC o zawartości 70% chromu na powierzchni stali AISI 1030 metodą PTA. W czasie nakładania powłoki zawartość azotu w gazie ochronnym wynosiła 1, 3, 5%. Uzyskane powłoki badane były za pomocą mikroskopii optycznej, skaningowej mikroskopii elektronowej, dyfrakcji rentgenowskiej i mikroanalizy rentgenowskiej. W oparciu o wyniki obserwacji i analiz mikrostruktury stwierdzono, że powłoka i warstwa pośrednia połączone są ze sobą metalurgicznie. Stwierdzono obecność austenitu, Fe-Cr, Fe<sub>23</sub>(C)<sub>6</sub>, Cr<sub>7</sub>C<sub>3</sub> oraz węglików i CrN w mikrostrukturze.

## 1. Introduction

Various surface processes are needed to protect metal surfaces from external environment or to eliminate or minimize fatigue, friction, and wear to which they are exposed according to their use area [1-3]. Plasma transferred Arc (PTA) has been widely used in welding surface process in coating engineering in recent years. In this method, coating powders are absorbed to molten bath with a separate powder feeding unit which was created with plasma transferred arc welding method on the surface of the material to be coated [4]. However, coating process is performed even by bonding coating powders on the surfaces of the material with special binders [5]. The coating process is performed by melting the powders with the energy given by the plasma transferred arc method [6]. Surface properties and quality depend on the coating process to perform the coating method and the selected alloys [7]. Therefore, surface coatings such as plasma transferred arc welding method and laser coat-

ing, which are performed by using high energy density welds are widely used in order to improve mechanical, corrosion, and tribological properties of surfaces [8-11].

Liu et al produced (Cr, Fe)<sub>7</sub>C<sub>3</sub> reinforced composite coatings by using Fe-Cr-C-Ni element powders on the surface of medium carbon steel with the plasma welding method [12]. Coating layers were produced by melting Fe-Ti alloy and B<sub>4</sub>C powders on the surface of low carbon steel [13]. The microstructures and mechanical properties of coating layers after solidification were significantly determined to have been affected by arc energy density and the amount, type, and size of the coating powder.

Yao et al. [14] examined corrosion-oxidation resistance as well as mechanical properties such as abrasion, adhesion and erosive wear of the coating material of the Co based Cr-W-C-Mo Stellite alloys they produced with the plasma transferred welding method. In their study, they determined that wear and corrosion resistance was quite better than the parent material owing to the pres-

\* UNIVERSITY OF FIRAT, FACULTY OF TECHNICAL EDUCATION, DEPARTMENT OF METALLURGY, 23119 ELAZIG, TURKEY

ence of over eutectic and near eutectic carbides in the microstructure of the coating layer.

Zhang et al [15] coated the surface of low carbon steel with Fe based alloys using the plasma transferred welding method and examined the characteristics of the produced coating layer. Austenite and hypereutectic structures were obtained on the coating layer.  $(Fe,Cr)_7(C, B)_3$  and  $(Fe,Cr)_3C_2$  were obtained with dendritic austenite  $\gamma$ -Fe in the primary phases of the coating layer.  $\gamma$ -Fe phase is an unstable solid solution phase. It was determined in abrasive wear test results of Fe based coating layer that wear resistance of the coating layer was much higher than that of low carbon steel. This was caused by dispersed dendritic austenites, hard carbides and borides. The maximum microhardness of the coating layer came out to be 780 HV.

Liu et al [16] examined adhesive wear resistance and microstructures of  $(Cr,Fe)_7C_3/\gamma$ -Fe ceramic composite coatings performed with PTA method. In the study, FeCrC was coated on the 0.45% C steel surface as the sub-layer with the PTA method. Rapidly hardening ceramic secondary dendrites  $(Cr, Fe)_7C_3$  and eutectic phases containing  $(Cr,Fe)_7C_3/\gamma$ -Fe among dendrites occurred on the coating layer. The coating process was performed at 120 A and Ar atmosphere. Because of the presence of  $M_7C_3$  and  $M_7C_3/\gamma$  phases occurred in the process, the wear resistance of the coating layer came out to be relatively high. The wear behaviour of the coating layer came out to be 35 times higher than that of the substrate, steel with 0.45% Cu. In addition, maximum microhardness of the coating layer came out to be about 850 HV.

Nitriding or carbonitriding process improves the mechanical and wear behaviours of metals. Because especially TiN and Ti (C,N) increase the wear corrosion behaviour of coatings, they have become a great interest for researchers [17]. Shielding gases such as He, Ar and the mixed gases apart from these are odorless and colorless mono atomic gases which have chemically neutral character. Although they do not add any heat contribution to the process area during processes such as coating and welding, they affect the heat input to some extent. Inert shielding gases protect the coating bath and tungsten electrode from negative effects of the environment during PTA process. They do not react with tungsten electrode and molten metal bath which are in hot state during the process. Although they do not have a negative effect on the metal quality, they have a significant effect on speed of the process and quality of the welded joint [18-20].

In this study, a FeCrC composite layer was produced on the surface of AISI 1030 steel with the plasma transferred arc welding method. The coating layer was pro-

duced at the constant current value in Ar and Ar-N<sub>2</sub> shielding gas atmosphere. The interfaces of the coating layer and AISI 1030 steel and coating layer were analysed with optical microscope, scanning electron microscope (SEM) and X-ray analysis, and their microhardnesses were determined.

## 2. Experimental study

AISI 1030 steel in 60 mm×14 mm×10 mm measures was used as a sub-layer material in surface coating processes (Fig. 1). Before the plasma transferred arc coating method, the surfaces of the steel materials were cleaned with acetone and they were dried. Channels having 4 mm width and 0.5 mm depth were opened and after the coating powders were placed in the channels, they were perfused upon mixing with alcohol. FeCrC powders in 70% Cr proportion, whose chemical compounds are given in Table 1, were used as coating powders. SEM

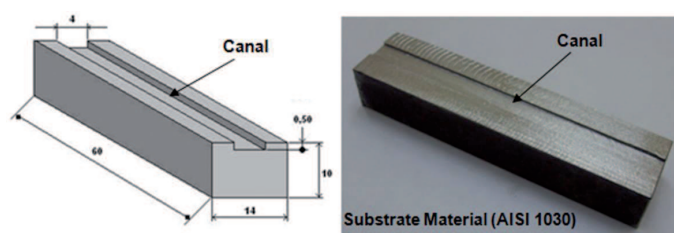


Fig. 1. Dimensional sample and canal opened of substrate material

TABLE 1

The chemical compositions of substrate and coating materials

	Weight (%) Composition							
	Cr	C	Fe	Ni	Si	Mn	W	Other
AISI 1030 Steel	18,57	0,035	Di.	8,73	0,40	1,24	–	–
FeCrC Powder	70.21	12.44	16.27	–	1.08	–	–	–

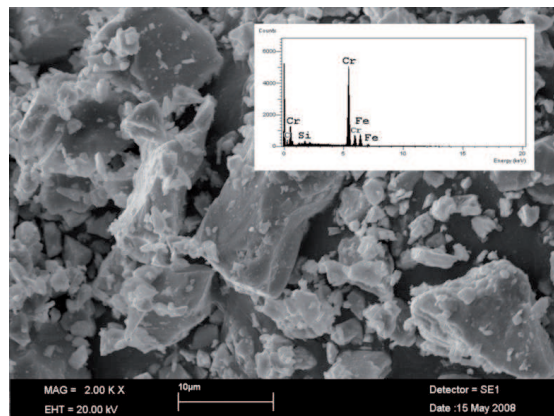


Fig. 2. The adhesive substance canal of powders

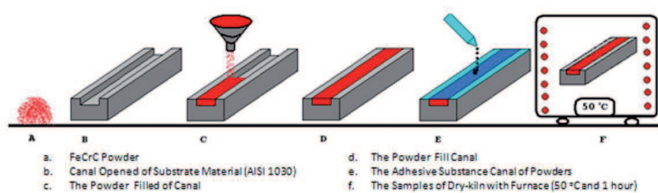


Fig. 3. Carbide and alloy powders used to manufacture coatings

image and EDS analysis used in the process are given in Fig. 2. In order not to let them move away from the perfused surface due to the flow rate of the shielding gas used in the PTA surface coating method, they were kept on the surface of the coating with a little binder and they were dried at 50°C for 1 hour (Fig. 3).

After the specimens were dried, the surface of the AISI 1030 material was alloyed in accordance with the parameters in Table 2 as in Fig. 4 with the PTA method. During this process, the first specimen A was alloyed in pure Ar atmosphere and the specimen B, the specimen C and specimen D were alloyed in pure Ar+1% N<sub>2</sub> atmosphere, pure Ar+3% N<sub>2</sub> atmosphere, and pure Ar+5% N<sub>2</sub> atmosphere, respectively.

TABLE 2

PTA weld-surfacing process experimental parameters and energy input

Samples	a	b	c	d
Arc current (A)			125	
Arc voltage (V)			17	
Shield gas flow (Ar, m <sup>3</sup> /h)	25 Ar	25 Ar+%1N <sub>2</sub>	25 Ar+%3N <sub>2</sub>	25 Ar+%5N <sub>2</sub>
Plasma gas flow (Ar, m <sup>3</sup> /h)			0.5, Ar	
Diameter of electrode (mm)			4.8	
Electrode Kind	% 2 thoryum (Th), tungsten (W)			
Travel Speed (mm/s)			0.15	
Torch and Samples Distance (mm)			3≈4	
Torch Gap (mm)			3.25	
Set Back (mm)			3	
Heat Input (KJ) Q			8.5	
Energy Input (KJ) Q <sub>w</sub> η:0.55 [21]			4.675	

Schematic view of the process ensuring the N<sub>2</sub> (g) ↔ 2N (k) equity during the process performed with gas metal arc welding in Ar + N<sub>2</sub> gas environment is seen in Fig. 5 [21]. While the specimens are alloyed in Ar+%N<sub>2</sub> atmosphere, it is inevitable for N<sub>2</sub> in the welding atmosphere to penetrate molten metal bath because while

the radius of C atom is 0.77 Angstrom, the radius of N atom is 0.71 Angstrom.

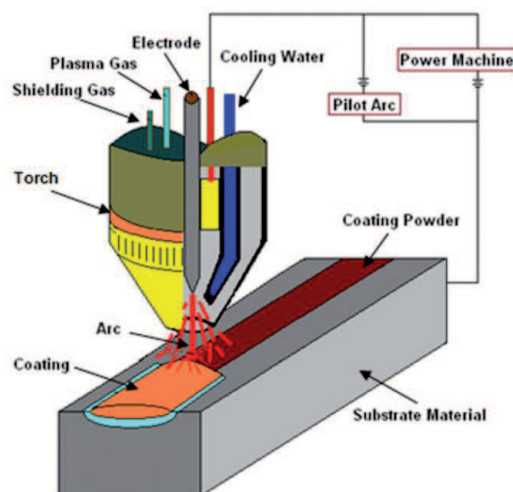


Fig. 4. Schematic appearance of PTA weld-surfacing process

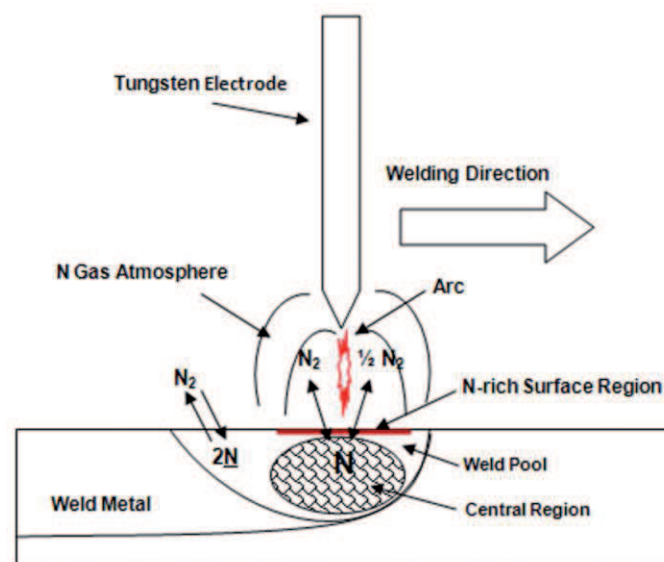


Fig. 5. A schematic illustration of the behavior of nitrogen during arc tungsten welding

Production parameters of the surface coating process performed with PTA method are given in Table 2. The surface coating processes with the plasma transferred arc welding method were performed at 125 A. While the flow rate of the Argon shielding gas was chosen as 25 l/min, the flow rate of the plasma gas was chosen as 0.5 l/min. Macro view of the coating material performed with the plasma transferred arc welding method is given in Fig. 6. No macro fracture was observed on the surface as a result of the solidification process after coating. For microstructure analyses, specimens in 10 mm×10 mm×10 mm size were taken from the middle region of the coating material (Fig. 7). The coating materials exposed to metallographic processes were etched in 5 gr FeCl<sub>3</sub>, 25 ml HCl, and 100 ml H<sub>2</sub>O solution for their microstructure analyses.

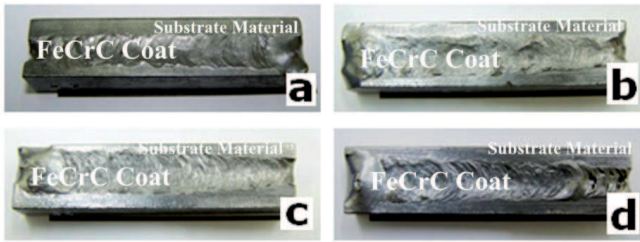


Fig. 6. Macrography of the surface-modified composite layer with FeCrC alloy powder on AISI 1030 steel

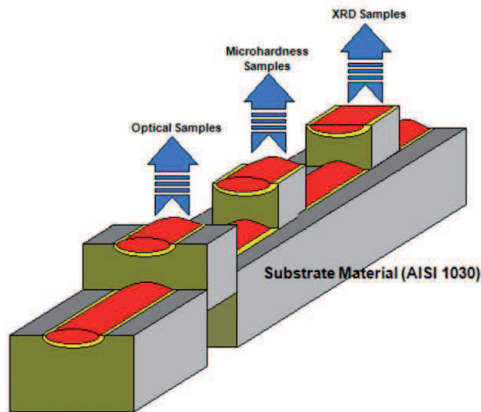


Fig. 7. The Extricate of Samples

While optical microscope (OM) scanning electron microscope (SEM) was used for microstructure analyses, X-ray diffraction (XRD) and X-ray energy dispersive spectrometer (EDS) were used for phase analyses. Microhardnesses of the coating layer were taken at 100  $\mu\text{m}$  distances from the coating surface to the sub-layer under 50 g load with Leica brand microhardness device.

### 3. Findings and Discussions

The thickness of the coating layer, which was formed on the surface of the AISI stainless steel with the plasma transferred arc method and whose optical image is given in Fig. 8, is  $1.6 \pm 0.2$  mm. A dendritic solidification occurred in the interface region between the coating layer and the substrate. The direction of the solidification was perpendicular to the interface of the coating substrate interface. The dendritic region occurred in approximately 450  $\mu\text{m}$  region in the coating layer. In the plasma transferred arc welding method, the energy which was given to both the surface and the coated powders and carbides was very high. Therefore, cooling and solidification speeds of the sub layer material, which was locally melted, and the coating material were also high.

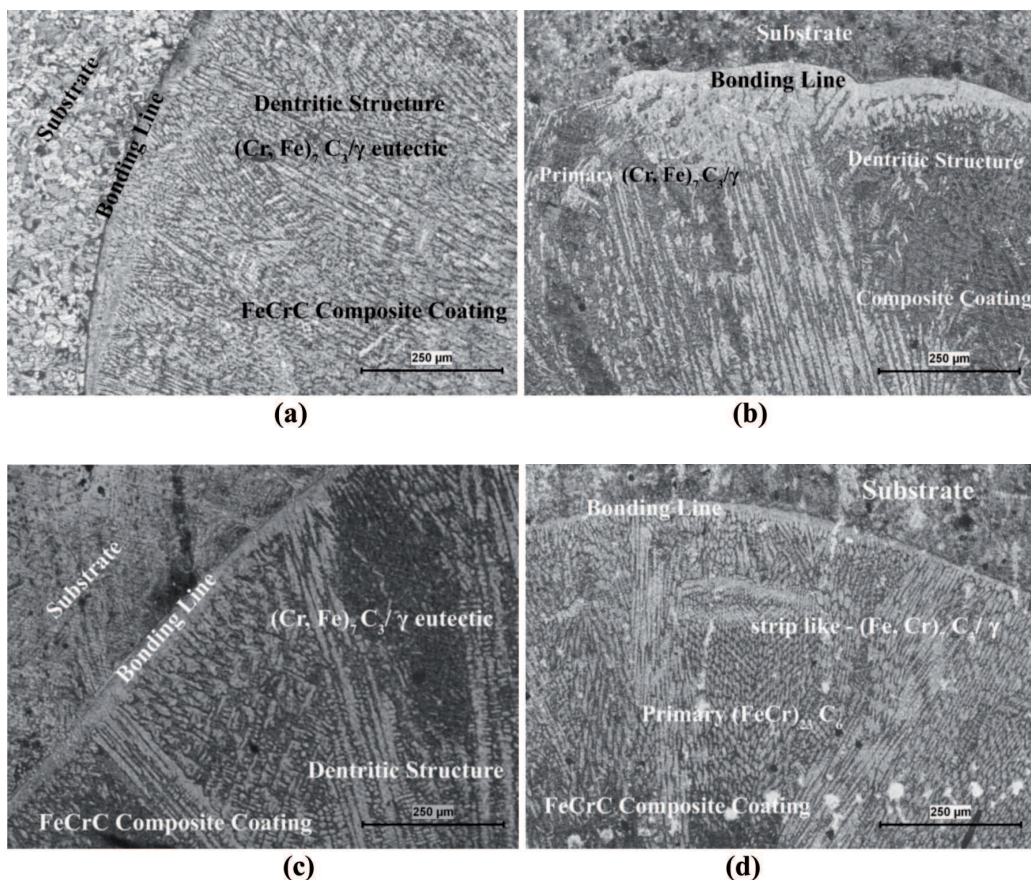


Fig. 8. Optical microstructures showing the metallurgical bonding of composite coatings to the AISI 1030 steel substrate with current values of (a) pure Ar atmosphere (b) Ar+1%  $\text{N}_2$  atmosphere, (c) Ar+3%  $\text{N}_2$  atmosphere (d) Ar+5%  $\text{N}_2$  atmosphere

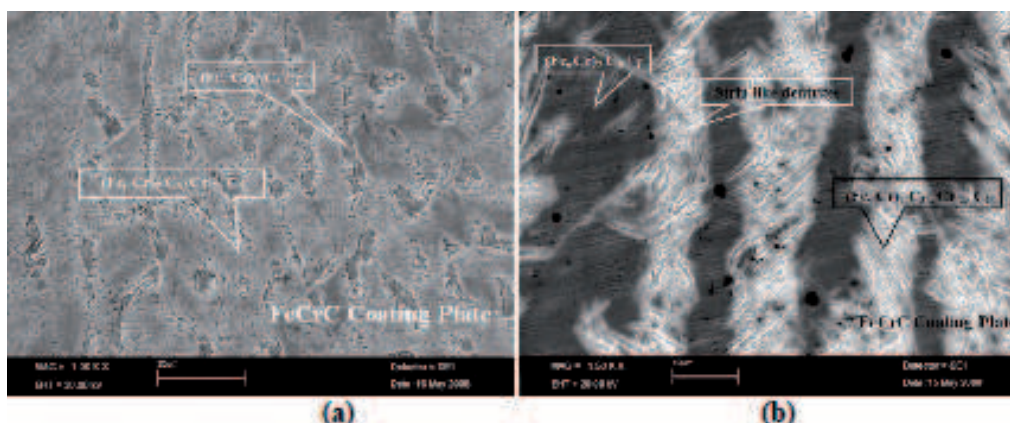


Fig. 9. SEM microstructure of plasma transferred arc surfacing cladding: (a) Ar+1% N<sub>2</sub> atmosphere, (b) Ar+3% N<sub>2</sub> atmosphere

Carbide and alloy elements dissolve at high temperature and they solidify by forming a new phase and carbides during solidification in the molten bath. When there is not enough temperature and time for the powder particles to dissolve, the particles solidify in blocks in the structure without dissolving in the molten bath [13]. As it is seen in Figure 8, in composite coating performed with FeCrC carbide and element powders, all powder particles dissolved completely and they showed a homogenous solidification in the structure.

Along the upper surface region of the coating layer, the dendritic structures turn to be phases and carbides that have a martensitic view. This state is given from the specimen B in SEM image in Figure 9 (a). The phases were surrounded with eutectic matrix. According to the EDS data obtained from the eutectic matrix, the structure having the compound of 13.00 Cr; 86.26 Fe; 0.51 Mn; 0.23 Si and the rest C and N showed solidification. If austenite is left to solidify at high temperatures, the structure will be formed with the structure having high concentrated Cr element and this structure will make the material more resistant to corrosion [14]. As it is seen in Figure 9 (a), the solidified phases in the eutectic phase

between dendrites are denser on the upper side of the coating layer in the structure. SEM image of the specimen C in high magnification of the carbide having needle martensite view is given in Figure 9 (b). The phases formed in the process solidified by absorbing relatively more C and N elements than eutectic matrix among dendrites. This structure formed as a result of rapid cooling turned out to have needle martensite view. According to the EDS analysis of the phase seen in Figure 9, the compound of the structure contains as % weight 19.33 Cr; 79.57 Fe; 0.86 Mn; 0.25 Si and the rest C and N. These needle martensitic phases dissolved homogeneously in blocks in the eutectic matrix. While EDS analyses were taken, because the atom relativistic masses of C and N are closer to each other, these values were not examined, but they were examined in the XRD results. With the addition of C in the C and FeCrC coating powder of the coated sub specimens, a high ratio of C passed on to the surface. In addition, with the addition of N gas which is added to the shielding gas and which can react with metals, it is inevitable that C having 0.77 Angstrom radius and N having 0.71 Angstrom radius form carbide and nitride on the coating layer.

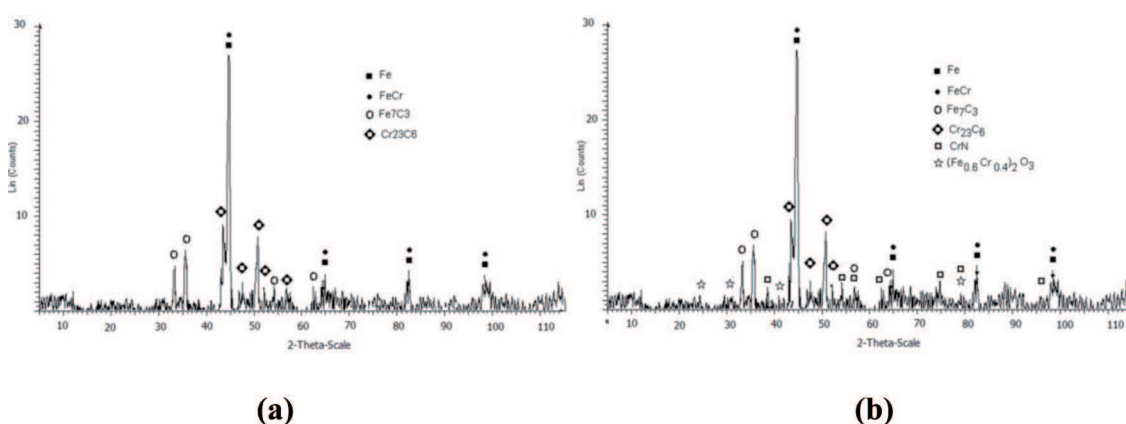


Fig. 10. XRD patterns of the composite coating produced by PTA weld-surfacing process: (a) pure Ar atmosphere, (b) Ar+5% N<sub>2</sub> atmosphere

X-ray diffractogram of the coating layer produced with FeCrC carbide-element powders is given in Fig. 10. X ray result indicates the presence carbides are also “phases” and on the coating layer obtained with FeCrC carbide-element powders by using the plasma transferred arc torch. The average values of hardness obtained from the coating layer of the FeCrC coated specimens came out to be a: 855, b: 880, c: 944 and d: 991 HV. Formation of CrN, FeCr ( $\sigma$ -phase),  $Fe_7C_3$ ,  $Cr_{23}C_6$  carbides, martensite and other hard phases on the coating layer was effective on why these values came out to be higher.

Although PTA method had high energy input advantage, it caused an increase in hardness in the alloyed region as it increased the penetration of  $N_2$  gas present in the shielding gas mixture, narrowed the matrix and formed CrN in the dendritic structure. In addition, because of the high carbon ratio of the ferrochromium powder, a dense carbon net occurred in the welding bath with the chrome which had a high carbide affinity.

The hardness began to increase with a little diffusion effect occurred under the coating layer starting from the coated material (Figure 11), and then a rapid hardness increase was observed in the interlayer as a result of the formation of carbide and nitride compounds, and the hardness reached up to 881-991 HV values beginning from approximately 0,2 mm distance from the interlayer [16]. As a result of homogenous dispersion carbides, nitrides and metallic compounds formed on the coating layer, the hardness dispersion in the layer happened in a completely balanced way.

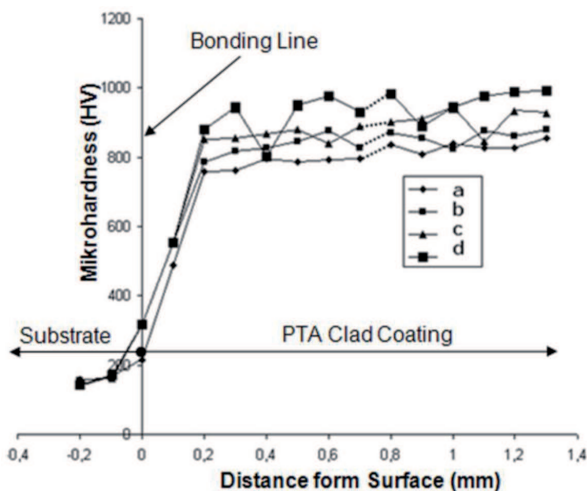


Fig. 11. Mikrohardness along the depth of the coating for the hard-facing track

#### 4. General results

By using the plasma transferred arc welding method, FeCrC carbide and element powders were successfully

melted on the surface of AISI 1030 steel. No macro and micro fracture occurred according to the macrostructure of the coating layer. All of the carbide and element powders used for surface coating were melted with plasma transferred arc energy, and austenite ( $\gamma$ ), CrN, FeCr ( $\sigma$ -phase),  $Fe_7C_3$ ,  $Cr_{23}C_6$  phases and carbides occurred in the microstructure after solidification. While the hardness of the substrate material was 170 HV, maximum hardness of the carbides was obtained as 991 HV from the specimen d. 12%C which was present at high ratio in the coating powder and 5%  $N_2$  in the shielding gas were effective on why hardness values came out to be so high. As a result, it was determined that the hardness of the coating layer in AISI 1030 steel was relatively higher than that of the sub-layer.

#### Acknowledgements

The author would like to acknowledge Firat University, Turkey for the financial support. (Project No. FUBAP-1470).

#### REFERENCES

- [1] K.H. Lo, F.T. Cheng, H.C. Man, Cavitation erosion mechanism of S31600 stainless steel laser surface-modified with unclad WC, *Materials Science and Engineering* **A357**, 168-180 (2003).
- [2] L. Bourithis, Ath. Milonas, G.D. Papadimitriou, Plasma transferred arc surface alloying of a construction steel to produce a metal matrix composite tool steel with TiC as reinforcing particles, *Surface and Coatings Technology* **165**, 286-295 (2003).
- [3] Shan-Ping Lu, Oh-Yang Kwon, Yi Guo, Wear behavior of brazed WC/NiCrBSi(Co) composite coatings, *Wear* **254**, 421-428 (2003).
- [4] Wang Xibao, Liu Hua, Metal powder thermal behaviour during the plasma transferred-arc surfacing process, *Surface and Coatings Technology* **106**, 2-3, 156-161, 4 August 1998.
- [5] L. Bourithis, G.D. Papadimitriou, The effect of microstructure and wear conditions on the wear resistance of steel metal matrix composites fabricated with PTA alloying technique, *Wear* **266**, 11-12, 1155-1164, 30 May 2009.
- [6] Wang Xibao, Li Chunguo, Peng Xiaomin, Shi Libo, Zhang Hong, The powder's thermal behavior on the surface of the melting pool during PTA powder surfacing, *Surface and Coatings Technology* **201**, 6, 2648-2654, 4 December 2006.
- [7] B. Vamsi Krishna, V.N. Misra, P.S. Mukherjee, Puneet Sharma, Microstructure and properties of flame sprayed tungsten carbide coatings, *International Journal of Refractory Metals and Hard Materials* **20**, 5-6, 355-374 December 2002.

- [8] Xiu-Bo Liu, Yi-Jie Gu, Plasma jet clad  $\gamma/\text{Cr}_7\text{C}_3$  composite coating on steel, *Materials Letters* **60**, 5, 577-580 March 2006.
- [9] P. Skarvelis, G.D. Papadimitriou, Plasma transferred arc composite coatings with self lubricating properties, based on Fe and Ti sulfides: Microstructure and tribological behavior, *Surface and Coatings Technology* **203**, 10-11, 1384-1394, 25 February 2009.
- [10] E. Bourithis, A. Tazedakis, G. Papadimitriou, A study on the surface treatment of "Calmax" tool steel by a plasma transferred arc (PTA) process, *Journal of Materials Processing Technology* **128**, 1-3, 169-177, 6 October 2002.
- [11] Zhenyi Huang, Qingyu Hou, Ping Wang, Microstructure and properties of  $\text{Cr}_3\text{C}_2$ -modified nickel-based alloy coating deposited by plasma transferred arc process, *Surface and Coatings Technology* **202**, 13, 2993-2999, 25 March 2008.
- [12] Yuan-Fu Liu, Zhi-Ying Xia, Jian-Min Han, Gu-Ling Zhang, Si-Ze Yang, Microstructure and wear behavior of  $(\text{Cr,Fe})_7\text{C}_3$  reinforced composite coating produced by plasma transferred arc weld-surfacing process, *Surface and Coatings Technology* **201**, 3-4, 863-867, 5 October 2006.
- [13] Wang Xibao, Wang Xiaofeng, Shi Zhongquan, The composite Fe-Ti-B-C Coatings by PTA powder surfacing process, *Surface and Coatings Technology* **192**, 2-3, 257-262, 21 March 2005.
- [14] M.X. Yao, J.B.C. Wu, W. Xu, R. Liu, Metallographic study and wear resistance of a high-C wrought Co-based alloy Stellite 706K, *Materials Science and Engineering: A* **407**, 1-2, 291-298, 25 October 2005.
- [15] L. Zhang, D. Sun, H. Yu, H. Li, Characteristic of Fe-based Alloy Coating Produced By Plasma Cladding Process, *Materials Science and Engineering A* **457**, 319-324 (2007).
- [16] Y.F. Liu, J.M. Han, R.H. Li, W.J. Li, X.Y. Xu, J.H. Wang, S.Z. Yang, Microstructure and dry-sliding wear resistance of PTA clad  $(\text{Cr, Fe})_7\text{C}_3/\gamma\text{-Fe}$  ceramal composite coating, *Applied Surface Science* **252**(20), 7539-7544 (2006).
- [17] M. Darabara, L. Bourithis, S. Diplas, G.D. Papadimitriou, ATiB2 metal matrix composite coating enriched with nitrogen: Microstructure and wear properties *Applied Surface Science* **254**, 4144-4149 (2008).
- [18] A.K. Gür, The Effect Of Shielded Gases at Surface Modification of Low Carbon Steel Alloys With Plasma Transferred Arc (PTA) Method, PhD Thesis, Firat University, Elazig, TURKEY (2009).
- [19] S. Anık, *Welding Technology Handbook*, Ergür Press., İstanbul, TURKEY (1983).
- [20] A.K. Gür, T. Yildiz, The Effect at Wear Behavior Of Coating Layer of Proportion Gases  $\text{N}_2$ ", *e-Journal of New World Sciences Academy*, **3**(4), 627-635 (2008).
- [21] T. Kuwana, H. Kokawa, M. Saitome, Quantitative prediction of nitrogen absorption by steel during gas tungsten arc welding, 3<sup>rd</sup> International Seminar on the Numerical Analysis of Weldability, Graz-Seggau, Austria, 25-27 September Mario (1995).
- [22] Marcioni, Plasma Arc Welding – (Energy input=  $\eta:0.55$ ) Lezione 1 – Il Plasma Ad Arco, Plasma Team Snc, Genova, 30 Giugno 2005. Istituto Italiano della Saldatura, pp. 41 (2005).